6.2. SSC 50 mm Aperture Collider Dipole Magnet Cross-section

In this section the magnetic design of the two dimensional coil and iron cross section for the prototype 50 mm aperture main ring dipole magnet for the Superconducting Super Collider (SSC) is presented. Several prototype dipole magnets based on this design have been built at Brookhaven National Laboratory (BNL) and at Fermi National Accelerator Laboratory (FNAL). Except for a few minor differences (which will be discussed in more detail later), the magnetic design of the BNL and FNAL magnets is nearly the same. The computed values of the allowed field harmonics as a function of current, the quench performance predictions, the stored energy calculations, the effect of construction errors on the field harmonics and the Lorentz forces on the coil will be discussed. The yoke has been optimized to reduce the effects of iron saturation on the field harmonics. A summary of this design will also be presented.

6.2.1. Coil Design

The coil is made of two layers of superconducting cables. Some parameters of the cables used in the inner and outer layers are given in Table 6.2.1.

The coil is designed by placing the cables in such a way that they produce a field with a high degree of uniformity. This is done using the computer program PAR2DOPT [130] which uses analytic expressions for computing the field harmonics at the center of the magnet of coils in a circular $\infty\mu$ iron aperture. It also computes the peak field on the surface of the conductor.

A large number of configurations for the coil design were examined. The one selected has a total of 45 turns in each quadrant in two layers. The inner layer has 19 turns in four blocks (three wedges) and the outer has 26 turns in two blocks (one wedge). In the final selection of the optimized coil cross section, the peak field (the maximum magnitude of the magnetic field in the conductor) was also used as an important parameter in addition to the other magnetic and mechanical parameters. For the same transfer function, a coil design with a lower peak field will produce a magnet which will quench at a higher current. In a search for the optimum coil configuration, the number of wedges in the outer layer was kept at one whereas for the inner layer, solutions with a variable number of wedges were examined. The designs with two wedges in the inner layer were, in general, found to have a higher peak field or excessive harmonic content. For this reason, the design chosen

Table 6.2.1: Properties of the cables used in the SSC 50 mm dipoles. J_c gives the value of the critical current density which was used in the design calculations for the superconducting part of the wires (strands) and cables.

Cable parameters	Inner layer	Outer Layer
Filament diameter, micron	6.0	6.0
Strand diameter, mm	0.808	0.648
Strand $J_c(5T, 4.2K)$, A/mm^2	2750	2750
No. of strands	30	36
No. of strands $\times$ Strand Area, mm^2 (area of metal)	15.382	11.872
Cable $J_c(5T, 4.2K)$, A/mm^2	2612.5	2612.5
Cable width, bare, mm	12.34	11.68
Cable width, insulated, mm	12.51	11.85
Cable mid-thickness, bare, mm	1.458	1.156
Cable mid-thickness, insulated, mm	1.626	1.331
Cable area, bare, mm^2	17.99	13.50
Cable area, insulated, mm^2	20.34	15.77
Keystone, (max-min) thickness, mm	0.262	0.206

has three wedges in the inner layer. However, the present coil is optimized in such a way that the two wedges nearest to the pole in the inner layer are identical and symmetric. A symmetric wedge design has a lower chance of incorrect installation as compared to a non-symmetric wedge design. The final design with symmetric wedges has performance comparable to those that did not require the wedges to be symmetric. The wedge in the outer layer is close to symmetric and in fact, in magnets built at FNAL this wedge was also made mechanically symmetric, without changing its effective size in the coil.

The cross section of the optimized coil placed in the stainless steel collar is shown in Fig. 6.2.1.

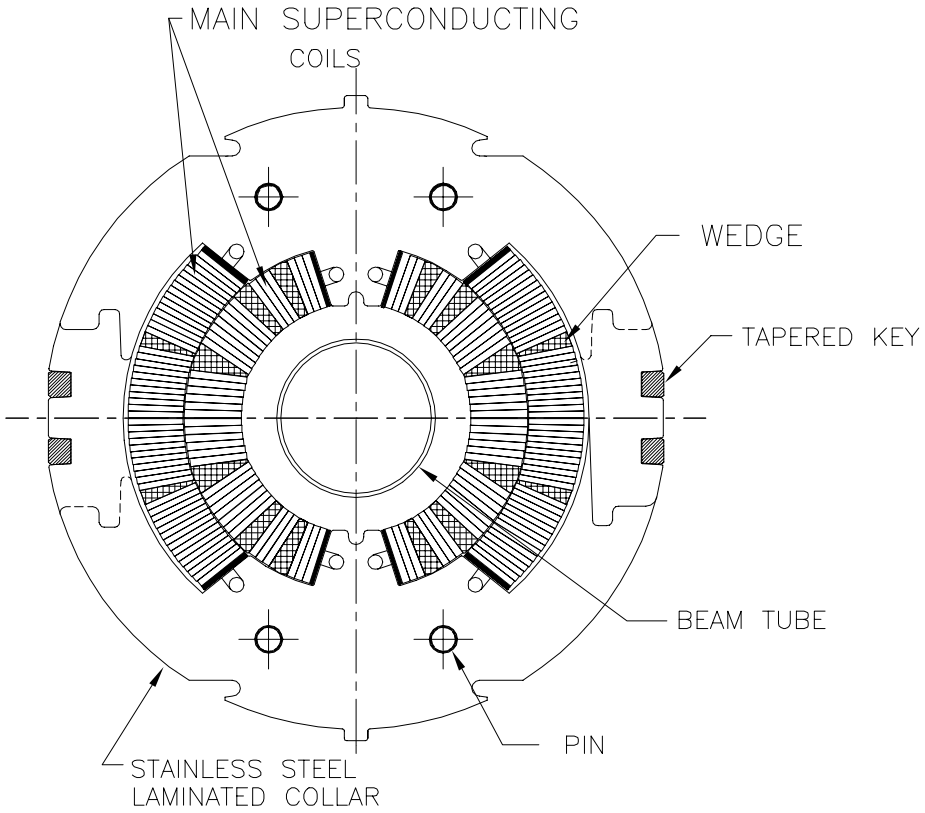

Figure 6.2.1: The cross section of the optimized coil for the prototype SSC 50 mm main collider dipole magnet. The coil is shown inside the stainless steel collar, which provides the compression on the coil.

6.2.2. Low Field Harmonics

The iron aperture is not completely circular in this magnet. It has a pole notch and a small vertical straight face at the midplane. These features introduce small but noticeable values of the b_2 and b_4 harmonics. These harmonics should be cancelled in the coil design if the magnet is to produce zero low field harmonics. Therefore, to cancel the effects of the non-circular iron inner radius, -0.28 unit of b_2 and $+0.01$ of b_4 were desired in the optimized coil. In addition, a non-zero value of b_8 harmonic was desired for centering the coil during the field measurements. Since the given tolerance in b_8 was 0.05 unit at the time of design, a solution was sought which had a magnitude for this harmonic between 0.04 and 0.05. This requirement on b_8 eliminated many coil configurations from contention. However, the final design that satisfied all of the above requirements was equal in performance to those that did not. An alternate cross section with a zero b_8 harmonic was also designed which was mechanically very close to this cross section and, moreover, had all wedges perfectly symmetric. However, no magnet was ever built with this alternate cross section.

In Table 6.2.2 the desired and optimized values of field harmonics are presented. Harmonics higher than b_{12} had an optimized value of < 0.001, as desired. In the row labelled "Desired" the allowed systematic errors are also listed. In the row "BNL magnets", the harmonics include the effects of the pole notch and the flat face in the iron at the midplane. These would be the expected values of low field harmonics in this magnet, not including the contributions from persistent currents in the superconductor. The size of the cable used in the actual magnets was different (inner layer cable wider and outer layer cable thinner) by a small amount from that assumed in the original design. This produced noteworthy deviations in the three lowest allowed field harmonics. The last two rows of the table, "Revised BNL" and "Revised FNAL", refer to the values of field harmonics in the magnet after this change in the cable size.

A small difference in the "Revised BNL" and "Revised FNAL" harmonics is due to the fact that (a) the pole angle in the outer layer of the FNAL cross section is 10 mil (0.254 mm) smaller than in the BNL version (the wedge size was the same therefore the effective cable thickness in the coil was reduced) and (b) the notch in the aperture of the vertically split iron is at the midplane and in the horizontally split iron is at the pole. The normalization or reference radius (R_0) for the field harmonics is 10 mm and as usual the harmonics are given in units 10^{-4} of the central field.

Table 6.2.2: Desired and Optimized values of *low field* harmonics with a circular aperture. The harmonics in "BNL magnets" include the effects of the pole notch and a flat face in the iron at the mid-plane. These harmonics are in units of 10^{-4} at 10 mm reference radius. The last two rows include the effects of a change in cable size.

Values	b_2	b_4	b_6	b_8	b_{10}	b_{12}
Desired	-.28±.4	.01±.1	0±.05	±.045±.05	0±.05	0±.05
Optimized	-0.280	0.009	-0.004	0.044	0.014	-0.001
BNL magnets	0.000	-0.001	-0.004	0.044	0.014	-0.001
Revised BNL	1.566	0.070	-0.024	0.043	0.015	-0.001
Revised FNAL	0.165	0.073	-0.021	0.043	0.015	-0.001

6.2.3. Iron Yoke Design

In this section, the process used in designing the iron yoke is discussed. The iron contributes about 22% to the magnetic field at 6.7 tesla (somewhat higher at lower field). Since the magnetization of the iron is not a linear function of the current in the coil and varies throughout the cross section, the uniformity of the field becomes a function of the current in the coil. The yoke is optimized to produce a minimum change in the field harmonics due to iron saturation for the maximum achievable value of transfer function at 6.7 tesla. The results of field computations with the computer codes POISSON and MDP will be presented here. The computer model of the final design and the results of field calculations with POISSON will be discussed in more detail. An iron packing factor of 97.5% has been used in these calculations.

If no special technique for controlling iron saturation were used, the change in the b_2 harmonic due to iron saturation would be over 1 unit. The following three options were considered for reducing the b_2 saturation swing. They all try to control the iron saturation at the iron aperture so that it saturates evenly.

- Reduced (shaved) iron o.d.
- Stainless Steel (non-magnetic) key at the midplane
- Shim at the iron inner surface

The first scheme, though most straight forward, produces a larger loss in transfer function at 6.7 tesla than the other two schemes. The third scheme, though actually increasing the transfer function at 6.7 tesla due to extra iron, requires more engineering development due to its non-circular aperture. The second scheme produces very little loss in transfer function (0.3% at 6.7 tesla compared to a keyless or magnetic key version) for a comparatively large reduction in b_2 due to saturation ($\frac{3}{4}$ unit). Moreover, it has the advantage of giving a way to control the b_2 due to saturation by changing the location and/or size of the key without affecting the other parts of the magnet design. It may be pointed out that besides the change due to iron saturation, b_2 and the other harmonics are also a function of current because of the coil deformation due to Lorentz forces. This has been observed in several SSC 40 mm aperture dipole magnets [64]. If the measured change in the b_2 harmonic is more than desired (either due to saturation or due to coil motion due to Lorentz forces), then this could be a useful and convenient method of correction.

The cross section of the cold mass (coil, collar and yoke) for the BNL-built SSC 50 mm prototype dipole is shown in Fig. 6.2.2. The POISSON model of this optimized cross section is given in a previous chapter as Fig. 3.2.2. The cross section for the vertically split iron used by FNAL is shown in Fig. 6.2.3. The field lines at 6500 ampere are also shown in this figure. The iron i.d. is 135.6 mm; leaving a space of 17 mm for the collar, and the iron o.d. is 330.2 mm. The stainless steel key in the horizontally split yoke design is located at 91.4 mm and has a size of 12.7 mm $\times$ 12.7 mm. In the vertically split design for the FNAL-built magnet, a cutout at the horizontal midplane is incorporated to reduce iron saturation. The size and location of this cutout is the same as in the BNL yoke. As mentioned earlier, the iron aperture is not completely circular. The BNL yoke has a pole notch of size 5.11 mm $\times$ 2.67 mm and a vertical straight face at the midplane which starts at $x = 67.13$ mm. The FNAL yoke has both the notch at the midplane and a vertical face at the midplane. The FNAL yoke has an additional pin located below the bus slot. This pin is made of non-magnetic steel and produces a noticeable effect on iron saturation. Other features in the two yokes are shown in the above mentioned figures.

The computed transfer function (T.F.) and b_2 as a function of current in the BNL and FNAL magnets are listed in Table 6.2.3. The b_2 harmonic has been adjusted so that it starts from zero; a non-zero value is artificial and is related to the way the computer model of a given coil and the iron geometry is set up in the two codes. The maximum computed b_2 due to saturation is about 0.3 unit. The calculations presented here, however, do not include

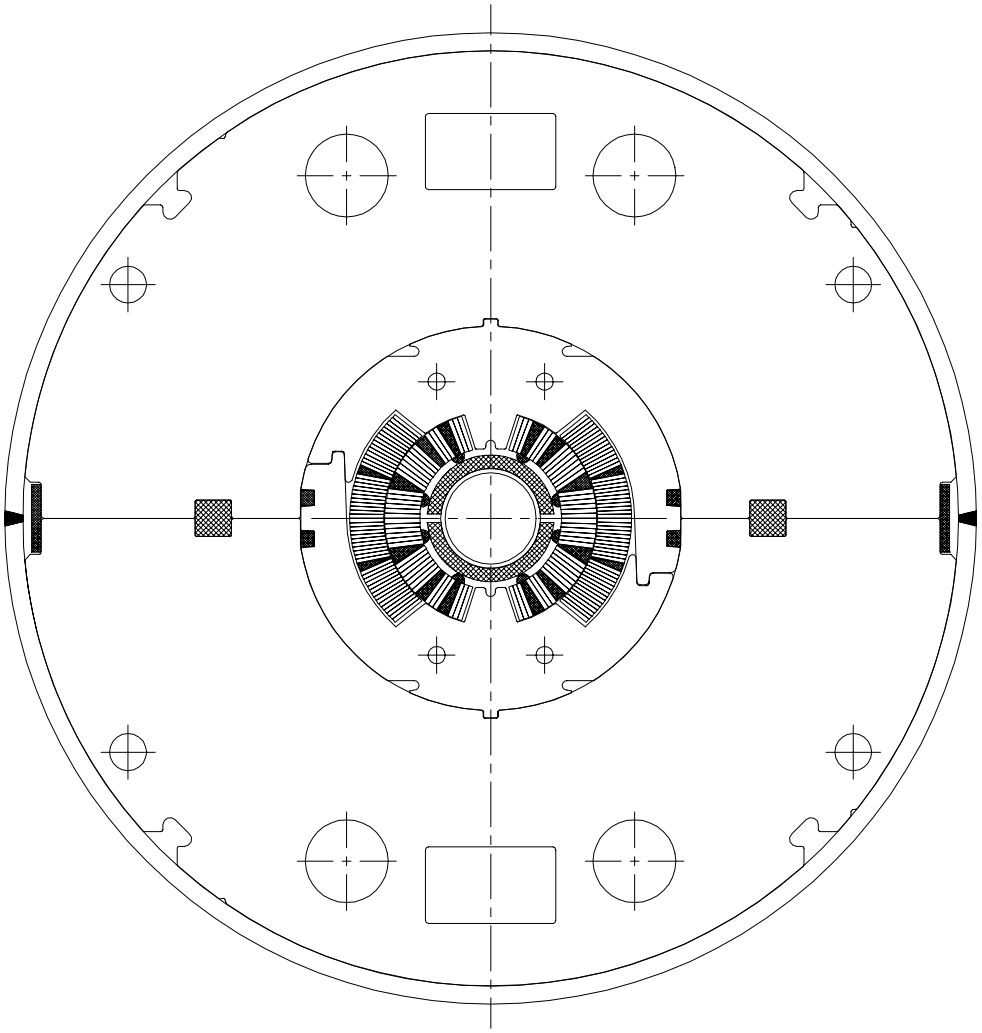

Figure 6.2.2: The cross section of the cold mass of 50 mm aperture horizontally split iron SSC arc dipoles. This cross section has been used in BNL built prototype magnets for SSC. The above cold mass is put inside a cryostat (not shown here).

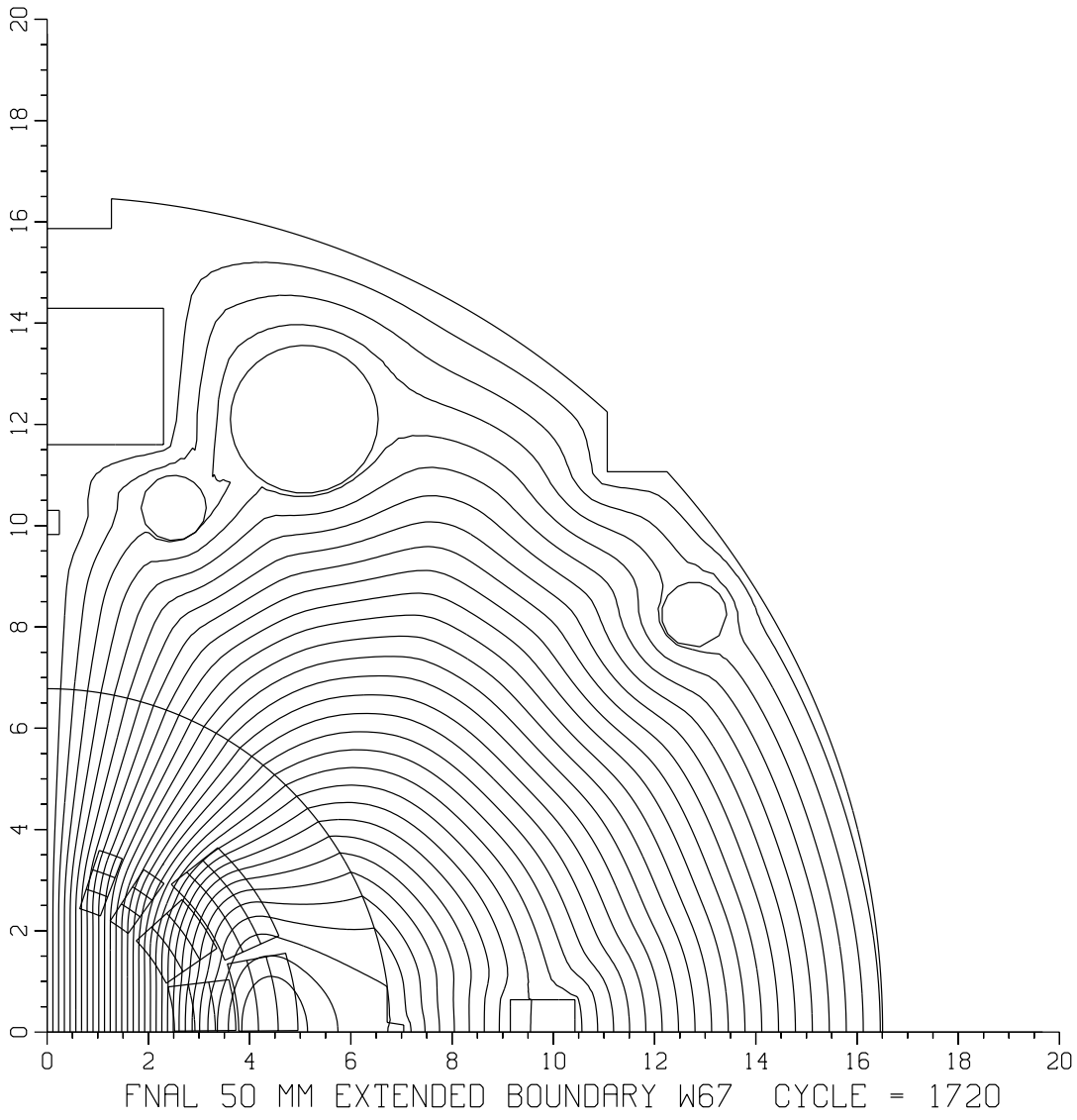

Figure 6.2.3: POISSON model and field lines at 6500 ampere for SSC 50 mm Dipole with vertically split iron laminations. This magnetic design was used in the prototype magnets built at FNAL.

the effects of the cryostat wall which modifies the current dependence of the harmonics at high current. POISSON uses a generalized finite difference method whereas MDP uses an integral method. Despite the fact that these two programs use two different methods for solving the problem, it is encouraging to see that both predict a small saturation shift. Similar calculations have been made by Kahn [64] with the computer code PE2D which uses the finite element method and good agreement has been found with the above calculations.

Table 6.2.3: Transfer function and b_2 variation as function of current. In all cases b_2 is corrected to start from zero at 3.0 kA. FNAL yoke calculations were done only with the code POISSON.

I	T.F. (T/kA)			$b_2 \times 10^{-4}$		
kA	FNAL	BNL yoke		FNAL	BNL yoke	
	yoke	POISSON	MDP	yoke	POISSON	MDP
3.0	1.0450	1.0447	1.0430	0.00	0.00	0.00
4.0	1.0445	1.0441	1.0413	-0.02	0.08	0.05
5.0	1.0398	1.0397	1.0364	-0.04	0.22	0.16
5.5	1.0339	1.0340	1.0311	0.19	0.26	0.21
6.0	1.0257	1.0262	1.0236	0.36	0.14	0.17
6.25	1.0209	1.0219	1.0194	0.38	0.07	0.11
6.5	1.0159	1.0173	1.0148	0.35	-0.03	0.03
7.0	1.0053	1.0073	1.0051	0.17	-0.33	-0.19
7.6	0.9926	0.9955	0.9935	-0.15	-0.77	-0.60
8.0	0.9845	0.9877	0.9861	-0.38	-1.06	-0.85
8.6	0.9732	0.9766	0.9758	-0.70	-1.43	-1.20

The maximum change in the b_2 and b_4 harmonics and the drop in transfer function, $\delta(TF)$, at 6.6 tesla (as compared to its value at low field) due to iron saturation as computed by these codes are listed in Table 6.2.4. All higher harmonics remain practically unchanged. In the case of the FNAL yoke, the computations have been done only with the code POISSON.

Table 6.2.4: Drop in transfer function at 6.6 tesla and the maximum change in b_2 and b_4; higher harmonics remain practically unchanged.

Harmonic	POISSON FNAL yoke	POISSON BNL yoke	MDP BNL yoke
$\delta(TF)$, at 6.6T	2.84%	2.62%	2.70%
$\delta(b_2)_{max}$, 10^{-4}	0.36	0.28	0.22
$\delta(b_4)_{max}$, 10^{-4}	0.02	-0.03	-0.02

In Table 6.2.5 the results of POISSON calculations are presented for various values of current in the BNL design. In Fig. 6.2.4, the variation in field harmonics as a function of central field is plotted.

The coldmass (see Fig. 6.2.2) is placed in the cryostat. To provide the maximum space for the support posts which minimizes the heat leak, the cold mass is placed above the center of the cryostat, which breaks the top-bottom symmetry. At high field, when the field lines can not be contained in the iron yoke, the cryostat provides an extra return path for flux. A top-bottom asymmetry in the magnet structure is then seen in the magnetic field. The most prominent harmonic to reflect this asymmetry is the skew quadrupole (a_1) term. The presence of the skew quadrupole harmonic at high field and methods to minimize it have been discussed in a previous chapter.

Table 6.2.5: Results of POISSON computations for the SSC 50 mm dipole with the horizontally split yoke design built at BNL.

I kA	B_o tesla	T.F. T/kA	b_2 10^{-4}	b_4 10^{-4}	b_6 10^{-4}	b_8 10^{-4}	b_{10} 10^{-4}	b_{12} 10^{-4}
$\infty\mu$	$\infty\mu$	1.04493	0.020	-0.046	0.000	0.047	0.015	-0.001
3.000	3.1341	1.04471	0.031	-0.046	0.001	0.047	0.015	-0.001
4.000	4.1762	1.04406	0.111	-0.050	0.001	0.047	0.015	-0.001
4.500	4.6921	1.04268	0.140	-0.055	0.001	0.047	0.015	-0.001
4.750	4.9464	1.04135	0.182	-0.060	0.001	0.047	0.015	-0.001
5.000	5.1985	1.03969	0.255	-0.063	0.001	0.047	0.015	-0.001
5.250	5.4454	1.03721	0.299	-0.066	0.001	0.047	0.015	-0.001
5.500	5.6871	1.03402	0.291	-0.069	0.001	0.048	0.015	-0.001
5.750	5.9240	1.03027	0.235	-0.071	0.001	0.048	0.015	-0.001
6.000	6.1573	1.02621	0.172	-0.073	0.000	0.048	0.015	-0.001
6.250	6.3868	1.02189	0.100	-0.073	0.000	0.048	0.015	-0.001
6.500	6.6121	1.01725	-0.003	-0.072	0.000	0.048	0.015	-0.001
7.000	7.0513	1.00733	-0.300	-0.072	0.000	0.049	0.015	-0.001
7.600	7.5654	0.99545	-0.738	-0.070	0.000	0.049	0.015	-0.001
8.000	7.9014	0.98767	-1.032	-0.068	0.000	0.050	0.015	-0.001
8.600	8.3984	0.97656	-1.403	-0.064	0.000	0.050	0.015	-0.001

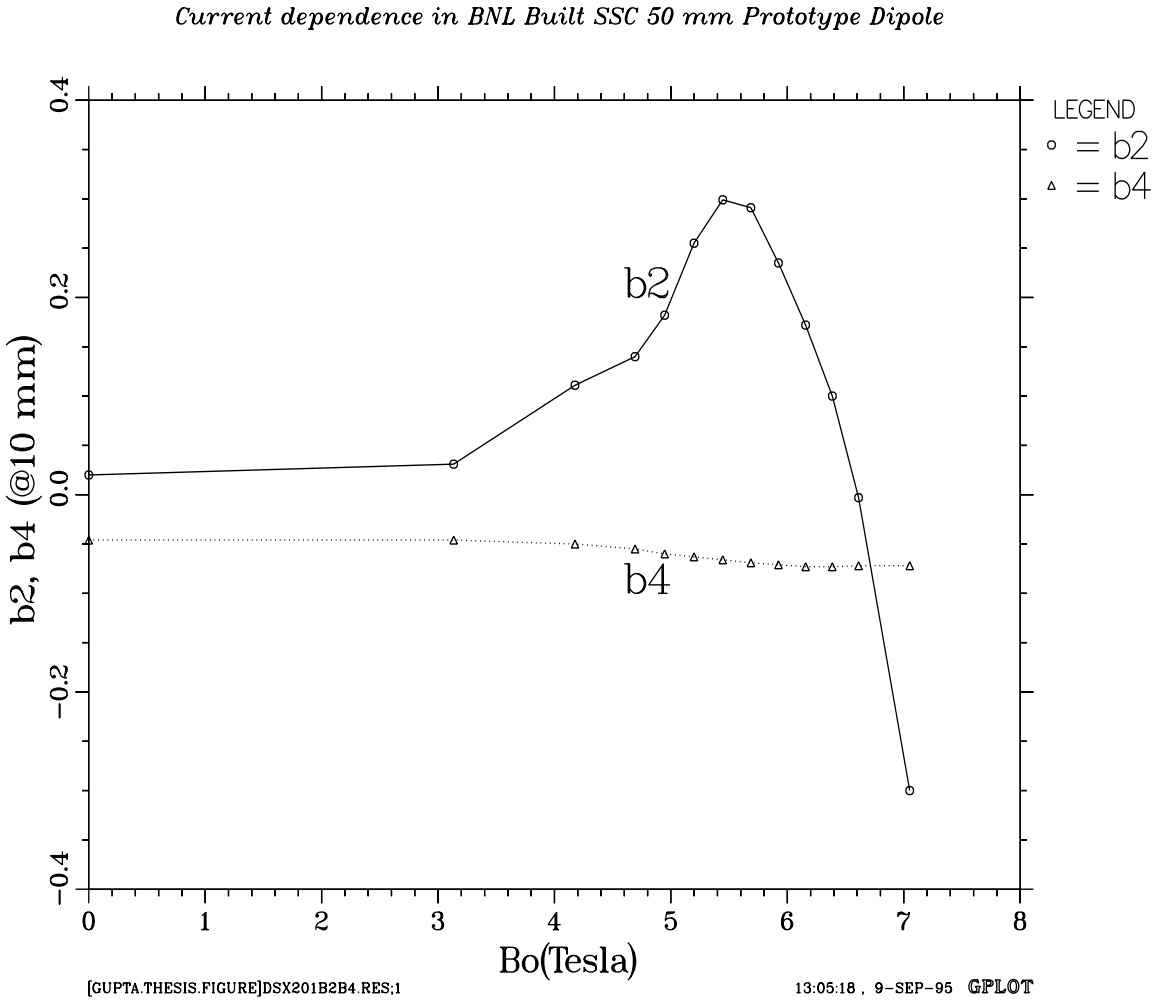

Figure 6.2.4: Variation in Field Harmonics as a function of Current in the SSC 50 mm BNL built prototype dipole magnet as computed by POISSON.

6.2.4. Expected Quench Performance

The central field at which a given cable looses its superconducting properties (B_{SS}, with "ss" standing for Short Sample) depends on the current in the cable which is a function of the maximum magnetic field at the conductor (the peak field) and the bath temperature. The superconducting cables for the inner and outer layers are optimized to provide a critical current (Ic) at a specified temperature and magnetic field. In a two layer coil design the magnetic design is optimized such that the computed short sample currents in the inner and outer layers are nearly the same. The peak field (B_{pk}) in the inner and outer layers of the SSC 50 mm dipole are listed in Table 6.2.6 for two values of central field (B_o). The ratio of B_{pk} to B_o, the *Enhancement Factor*, is given in the next column. In each layer, the peak field is found on the upper side of the top-most pole turn. The location of the peak field is listed in the next column. It is expressed as % of the cable width, measured from the upper-inner corner. The peak field calculations are done using the code MDP. MDP is based on the integral method and therefore is expected to give a more accurate field at the surface of the conductor as compared to codes based on the finite element method which require meshing the conductor.

Table 6.2.6: Peak fields in the SSC 50 mm dipole as computed using code MDP.

I	B_o	Inner			Outer		
kA	tesla	B_{pk},T	$\frac{B_{pk}}{B_o}$	Location	B_{pk},T	$\frac{B_{pk}}{B_o}$	Location
6.85	6.9058	7.2374	1.048	5%	6.0016	0.869	11%
7.20	7.2100	7.5595	1.048	5%	6.2660	0.869	11%

The calculations assume that the superconductor in the wire will have a critical current density $J_c(5T, 4.2K)$ of 2750 A/mm^2. The quality of the superconductor is degraded when the wires are made in to a cable and put in the magnet. The calculations presented in Table 6.2.7 have been done assuming 5% degradation (J_c=2612.5) and 4.35 K bath temperature.

In Table 6.2.7, the field margin (B_{margin}) and the temperature margin (T_{margin}) are listed. The temperature margin is defined as the maximum possible computed rise in the operating temperature (over the design value of normal operation, which is 4.35 K) before

Table 6.2.7: Expected quench performance of the SSC 50 mm dipole with 5% cable degradation ($J_c = 2612.5 A/mm^2$) and at 4.35 K temperature. S_{quench} is the computed current density in the copper at quench and $S_{6.7T}$ at the design field of 6.7 Tesla.

Layer ↓	Cu/Sc Ratio	B_{ss} tesla	I_c A	B_{margin} %over 6.7T	T_{margin} kelvin	S_{quench} A/cm^2	$S_{6.7T}$ A/cm^2
Inner	1.7	7.149	7126	6.7	0.519	736	681
	1.5	7.273	7273	8.6	0.625	788	715
	1.3	7.399	7411	10.4	0.730	853	759
Outer	2.0	7.268	7267	8.7	0.580	919	834
	1.8	7.445	7470	11.1	0.709	980	865

the magnet will quench at the design central field (B_{design}=6.7 tesla). The field margin is defined as follows

$$B_{margin}\,(\%) = \frac{B_{ss} - B_{design}}{B_{design}} \times 100$$

The calculations are done for copper to superconductor ratios, CSR or Cu/Sc, of 2.0 and 1.8 in the outer layer and 1.7, 1.5 and 1.3 in the inner layer. The computed central field (B_{ss}) at the magnet quench point is listed together with the current in the cable at that point (I_c) and the current density (S_{quench}) in the copper available to carry that current after quench. A lower current density in the copper is expected to give better stability. The current density in the copper at 6.7 tesla ($S_{6.7T}$) is also listed. For stability purposes, $S_{6.7T}$ may be a more appropriate parameter to consider than S_{quench}.

The design values selected were a copper to superconductor ratio of 1.8 in the outer layer and of 1.5 in the inner layer. The quench field B_{ss} of 7.273 tesla in the inner layer gives a field margin of 8.6% over the design operating field B_{ss} of 6.7 tesla. The quench field of 7.445 tesla in the outer layer gives a field margin of 11.1%.

6.2.5. Effect of Manufacturing Errors on the Allowed Harmonics

For various reasons, the actual value of a parameter used in designing the coil may turn out to be somewhat different than desired. In particular, deviations in the locations of various turns in the coil are very important. This causes changes in the transfer function and the field harmonics. In this section the effect of these errors in various cases are estimated using a procedure developed by P.A. Thompson [130]. The basic four fold symmetry in the dipole coil geometry is retained in this analysis. Though this is not a realistic assumption, it is useful in estimating the size of some errors. In Table 6.2.8 these effects are listed for a nominal 0.05 mm variation in the given parameter.

First, the change in harmonics due to a change of $+0.05$ mm in the radius of every turn in each current block, one block at a time, is given. The counting of the blocks in the table starts at the inner layer and at the midplane of each layer. Next the effect of changing the wedge size by $+0.05$ mm is estimated. Pole angle is held constant in this calculation by reducing the conductor thickness by an appropriate amount. The counting scheme for the wedges is the same as it is for the current blocks. It is possible that during the molding, the thickness of the cable is not reduced uniformly within a layer. To estimate this effect, a linear increase in the cable thickness is assumed going from the midplane towards the pole, followed by a linear decrease, such that the middle turn is displaced azimuthally by 0.05 mm. The pole angle does not change during this perturbation. This effect is given for the inner and outer layers in the next two rows of the table. The effect of increasing the pole angle by 0.05 mm in the inner and in the outer layer is shown in the last two rows. In each group the Root Mean Square (RMS) change of these variations is also given.

Table 6.2.8: The effect of a 0.05 mm increase in the given parameter on the transfer function and the field harmonics.

Parameter changed	TF T/kA	b_2 10^{-4}	b_4 10^{-4}	b_6 10^{-4}
Radius of Block No. 1	0.31	-0.25	-0.10	-0.01
Radius of Block No. 2	-0.32	0.31	0.12	0.01
Radius of Block No. 3	-0.12	0.36	-0.02	-0.01
Radius of Block No. 4	-0.20	0.33	-0.08	0.01
Radius of Block No. 5	-0.11	-0.04	-0.01	0.00
Radius of Block No. 6	-0.78	0.22	0.03	0.00
RMS Blocks	0.38	0.27	0.07	0.01
Thickness of Wedge No. 1	-1.56	-0.48	0.02	0.01
Thickness of Wedge No. 2	0.83	0.59	0.05	-0.01
Thickness of Wedge No. 3	2.32	0.71	-0.04	0.00
Thickness of Wedge No. 4	-0.57	-0.11	0.00	0.00
RMS Wedges	1.48	0.52	0.03	0.01
Cable thickness inner	2.63	1.08	0.05	-0.01
Cable thickness outer	1.99	0.48	0.02	0.00
RMS Cable thickness	2.33	0.83	0.04	0.01
Pole angle inner	-4.01	-0.45	0.06	-0.01
Pole angle outer	-2.26	-0.42	0.00	0.00
RMS Pole angles	3.25	0.43	0.04	0.01

6.2.6. Stored Energy and Inductance Calculations

Stored energy calculations are done with the computer code POISSON [135]. POISSON uses the following formula to compute the stored energy per unit length (E_l) over the cross section area :

$$E_l = \tfrac{1}{2} \int_a J \ A_z \ da,$$

where A_z is the vector potential and J is the current density in the mesh triangle having an area da. The integration needs to be performed only over the regions containing current. At low fields when the field B is proportional to I (i.e. when yoke saturation is not significant), the stored energy is expected to be proportional to B^2 or I^2.

The stored energy and the inductance are related through the following formula :

$$Stored \ Energy = \tfrac{1}{2} Inductance \times (Current)^2.$$

The inductance decreases at high field as the iron yoke saturates.

The results of POISSON computations for the SSC 50 mm aperture dipole are given at 6.5 kA in Table 6.2.9 for the stored energy per unit length and the inductance per unit length. The total stored energy and the inductance for a 15 m long dipole are also given.

Table 6.2.9: Stored Energy and Inductance at 6.5 kA as computed with the code POISSON for the SSC 50 mm aperture dipole.

Stored Energy per unit length, kJ/m	105.0
Stored Energy for 15 m long Dipole, kJ	1575.6
Inductance per unit length, mH/m	4.972
Inductance for 15 m long Dipole, mH	74.585

6.2.7. Lorentz Force Calculations

The value of Lorentz force per unit of axial length on each turn is obtained from the components of the magnetic field (B_x, B_y). These components are calculated using program MDP. Since B_x and B_y are not uniform in a turn, an average value of these components is obtained from a grid of 10×2 across the width and thickness of the cable.

The variation in the magnitude of the radial and azimuthal components of the Lorentz forces, namely F_r and F_a (also referred to as F_θ), with turn number is shown in Fig. 6.2.5. The turn numbers are counted from the midplane. The Lorentz force acts on the coil such that the azimuthal component compresses the coil on the midplane and the radial component expands it outward. Though the radial Lorentz force on the turns in the outer layer is very small, the force on the turns in the inner layer must be transmitted through the outer layer to the structure of the magnet.

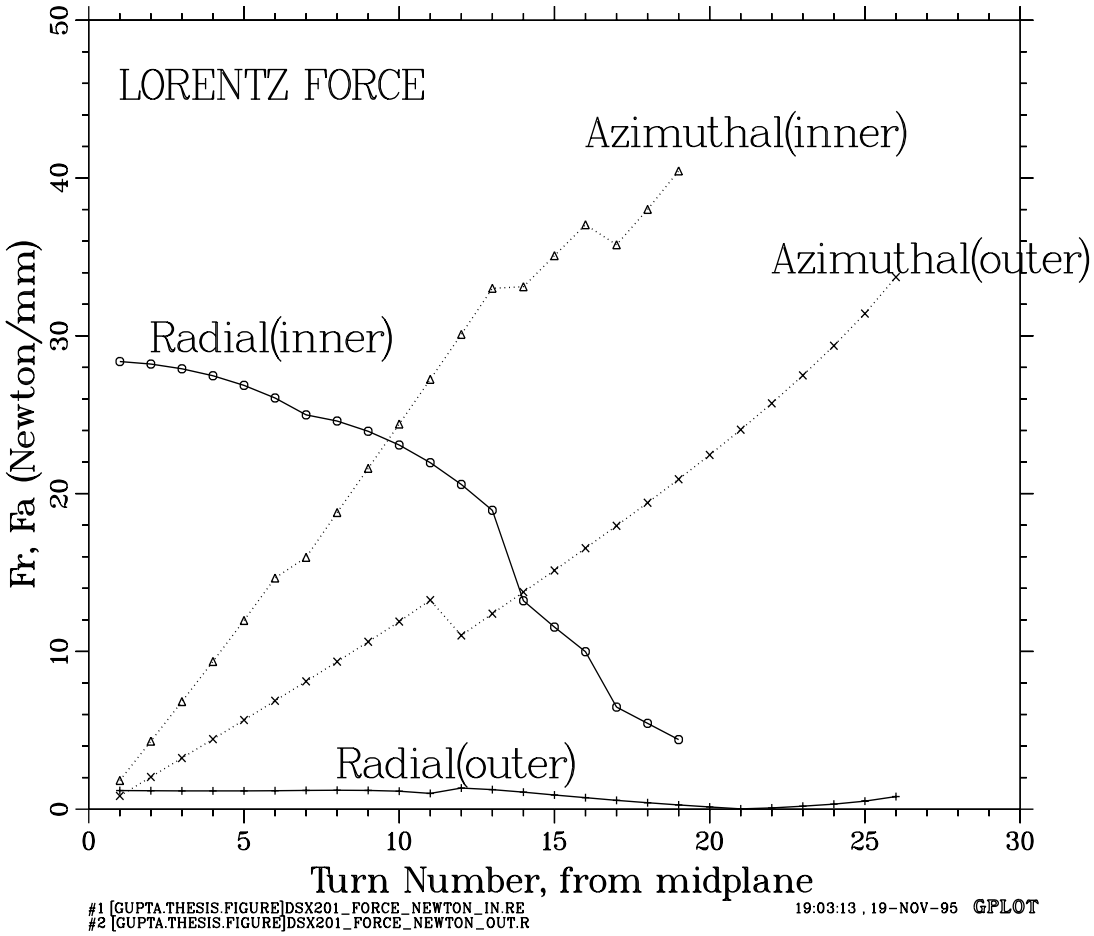

Figure 6.2.5: The magnitude of the components of the Lorentz force on the individual turns in a SSC 50 mm prototype magnet. The radial component of the force (F_r) pushes the coil outward and the azimuthal component (F_a) compresses the coil towards the midplane (horizontal plane). There are 19 turns in the inner layer and 26 turns in the outer layer of each quadrant.

6.2.8. Summary of the Design

A summary of the coil and iron cross-sections are given respectively in Table 6.2.10 and Table 6.2.11. The coil has two layers and the number of turns is the number of turns in the upper or lower half of a layer. The field margin in this cross section is limited by the inner layer. If the cable used in the inner layer had a copper to superconductor ratio of 1.3, the margin would be 10.4% (see Table 6.2.7).

Table 6.2.10: Summary of SSC 50 mm dipole coil cross section.

Layer →	Inner	Outer
No. of Turns	19	26
Strand Diameter, mm	0.808	0.648
Strands per turn	30	36
Coil i.d., mm	49.56	74.91
Coil o.d., mm	75.36	99.42
B_{peak}/B_o	1.048	0.869
Cu/SC	1.5	1.8
Margin over 6.7 T ...	8.6%	11.1%

Table 6.2.11: Summary of SSC 50 mm dipole iron cross section. $\delta(TF)$ is the change in transfer function, δb_2 in b_2 and and δb_4 in b_4 due to saturation.

Inner Diameter, mm	135.6
Outer Diameter, mm	330.2
$\delta(TF)$, at 6.7 T	2.6%
δb_2, prime unit	0.3
δb_4, prime unit	0.03